Evaluation of the Lapillar Otolith Shape as a Tool for Discrimination of Stock of Naked Carp, *Gymnocypris selincuoensis* in the Tibetan Plateau

Kang Chen[1,2], Dekui He[1], Chengzhi Ding[3,4], Yintao Jia[1] and Yifeng Chen[1]*

[1]Laboratory of Biological Invasion and Adaptive Evolution, Institute of Hydrobiology, Chinese Academy of Sciences, 430072, Wuhan, China

[2]University of Chinese Academy of Sciences, Beijing 100049, China

[3]Institute of International Rivers and Eco-security, Yunnan University, Kunming, Yunnan 650091, China

[4]Yunnan Key Laboratory of International Rivers and Transboundary Eco-Security, Yunnan University, Kunming 650091, China

ABSTRACT

Otolith geographic variability is investigated as a tool for fish stock discrimination. Despite increasing studies of otoliths in marine ecosystems, feasibility of otolith shape as an investigative tool in freshwater fish assemblages needs to be validated. The aim of this study was to test stocks of *Gymnocypris selincuoensis* that may be distinguished using otolith shape from three rivers and eight lakes in northern Tibet. Shape indices (SDs) (form-factor, circularity, rectangularity, ellipticity, roundness, surface density and aspect ratio) and normalized Elliptic Fourier descriptors (NEFDs) were analysed by multivariate statistical procedures. To examine the differences of otolith shape from different sites, metric multidimensional scaling and a linear discriminant analysis were used for the SDs and NEFDs. The results of the linear discriminant analysis indicate that riverine otolith stocks had higher rates of successful classification compared with lacustrine otolith stocks, and stocks of otoliths from the Chargut Co and the Kyaring Co lakes had the highest rates of misclassification. Although a 70% classification success rate was produced by Bochu Tsangpo, the differences in otolith shape among 11 stocks were not very noteworthy. The information generated in this research can be used as a reference for stock discrimination of *G. selincuoensis* from the Tibetan Plateau. Further research is needed to explore the causes of shape variation.

INTRODUCTION

Studying fishery stock structure plays an important role in fishery assessment and understanding the population dynamics of a species in an ecological sense (Begg *et al.*, 1999; Neves *et al.*, 2011; Stransky *et al.*, 2008b; Tracey *et al.*, 2006). Population units of fish have unique growth and reproduction characteristics (Bacha *et al.*, 2016). Currently, a series of techniques are used for fish stock discrimination, including morphological analyses, genetic markers, life-history traits, otolith shape and elemental analyses (Avigliano *et al.*, 2017; Begg *et al.*, 1999; Ihssen *et al.*, 1981; Secor, 2013). Among the techniques that are based on phenotypic variations, geometric analyses were applied frequently for fish stock discrimination, as they can be measured directly and compared easily,

especially for intraspecific semi-discrete stocks that cannot be separated clearly by genetic data (Bacha *et al.*, 2014; Cañás *et al.*, 2012; Soeth *et al.*, 2019). Nevertheless, many physical traits, such as body shape, otolith shape and scale shape (Neves *et al.*, 2011; Stransky *et al.*, 2008b) have been used to distinguishing fish populations. Otoliths are calcareous organizations located underneath the braincase and grow during the entire life of a fish. Otoliths possess stock specific characteristics which are associated with genetic heterogeneity and environmental factors (Ihssen *et al.*, 1981). The shape of otolith was considerd the most reliable tool compared to others because its lacks dependence on short-term variability due to changes in somatic growth (Campana and Casselman, 1993; Campana *et al.*, 2000). In particular, previous studies on otolith geometrical morphology have shown that otolith shape analyses were useful in taxonomy and successful in interspecific and intraspecific discrimination (Begg *et al.*, 2001; Burke *et al.*, 2008; Campana and Casselman, 1993; Härkönen, 1986; Tuset *et al.*, 2006).

Otolith shape indices (SDs) and normalized elliptical Fourier descriptors (NEFDs) of contours are two fundamental shape variables that are used frequently for fish stock discriminations. Comparing the two SDs are used to directly describe otolith frame structures in the form of manual distance measurements, whereas Elliptical Fourier analysis is deemed as useful tool for capturing outline information efficiently in a quantifiable manner (Avigliano *et al*., 2018; Kuhl and Giardina, 1982; Torres *et al*., 2000). Elliptical Fourier analyses have been widely used in identifying marine fish assemblages (Bird *et al*., 1986; Campana and Casselman, 1993), because of the advantages in accommodating significantly more complex shapes when compared with polar Fourier functions. However, SDs and NEFDs are generally combined for stock discrimination for improvement of classification success (Agüera and Brophy, 2011; Dou *et al*., 2012; Moreira *et al*., 2019; Tracey *et al*., 2006).

Despite the increasing studies of identifying fish stocks with otolith morphology throughout the world, feasibility of otolith shape in discriminating freshwater fish stocks needs more exploration (Bostanci *et al*., 2015). Different marine fish species have large pairs of sagittal otoliths and have frequently been used as materials for species identification (Campana and Casselman, 1993).In freshwater Cypriniformes, especially for Schizothoracine fishes, sagittal otolith cannot be used for morphological analysis because its special aciculiform shape makes its extracting and measurement difficult. Lapillar otoliths of Schizothoracine fishes have moderate size and stable shapes, which are generally used for studying life history (Chen *et al*., 2009; Jia and Chen, 2009; Li *et al*., 2009). However, there has been surprisingly little effort to use lapillar otoliths as study objects to identify discrete stocks on an intra-species scale (Assis, 2007; Bostanci *et al*., 2015; Campana and Casselman, 1993). The understanding of lapillar otolith shapes for stock discrimination is imperative for validation in freshwater ecosystems.

Schizothoracine fishes are group of Cyprinidae living in high elevation rivers and lakes in the Qinghai-Tibetan Plateau (Cao *et al*., 1981; Chen *et al*., 2001b). Schizothoracine species are characterized by restricted distributions, low growth rate, and late sexual maturity as a result of adapting to rigorous environment (Chen and Cao, 2000; Wu and Wu, 1992). Naked carp species (Genus *Gymnocypris*) are one of the specialized groups within Schizothoracines that belong to the subfamily Schizothoracinae of Cyprinidae (Chen and Cao, 2000) and are mainly distributed in the middle and upper reaches of rivers and lakes on the Tibetan Plateau with an elevation range of 1500 to 5000 m (Ding *et al*., 2015; He

and Chen, 2007). Numerous rivers and lakes constitute an enclosed basin system in northern Tibet, and naked carp species that were distributed in this system consist of multiple stocks (Chen *et al*., 2001b; Liang *et al*., 2017). Recent empirical studies made efforts to identify the fish stock by physical features; but, no evidence of separate stocks was found using external morphological characteristics or organ form features which could be used for fish stock classification (Liang, 2017; Wu and Wu, 1992). Molecular experiments of cytochrome *b* also demonstrated a low genetic differentiation among Schizothoracines (He *et al*., 2016; He and Chen, 2007). Therefore, these rivers and lakes are ideal sites for investigating the potential of using lapillar otolith shapes for identification of freshwater fish stocks.

Although otolith morphometrics have never been used in Schizothoracine fish, the moderate size and stable structure of lapillar otoliths allow them to potentially create two dimensional images that can be compared statistically (Jia and Chen, 2009). The aims of this study were to 1) evaluate the presence of lapillar otolith shape differences in different fish stocks of *G. selincuoensis* fishes, and 2) examine the utility of the lapillar otolith shape for stock discrimination in *G. selincuoensis* fishes.

MATERIALS AND METHODS

Study area and sample collection

The Qinghai-Tibetan Plateau possesses the highest lakes and rivers in the world; the total lake area exceeds 41,000 km^2 and accounts for approximately one half of the total Chinese lake area (Ma *et al*., 2011). Siling Co lake (88°33′ - 89°21′ °E, 31°34′ - 31°51′ °N) is located in northern Tibet (4300-7100 m above sea level) and is the largest lake in Tibet with an area of 2360 km^2 (Che *et al*., 2015). Lakes (Siling Co, Nagtsang Co, Chikul Co) and rivers (Tsachu Tsangpo, Chargut Tsangpo, Bochu Tsangpo) in northern Tibet are connected and constitute an enclosed basin system with various hydrological characteristics, such as temperature, depth and salinity (Bian *et al*., 2010; Chen *et al*., 2001a) (Fig. 1).

G. selincuoensis were collected from three rivers: the Bochu Tsangpo (BT), the Chargut Tsangpo (CT), and the Tsachu Tsangpo (TT), and eight lakes: the Siling Co (SC), the Nagtsang Co (NC), the Kyaring Co (KC), the Mokiu Co (MC), the Chargut Co (CC), the Uruni Co (UC), the Yoqag Co (YC) and the Chikul Co (CK) (Table I, Fig. 1). Collection was performed in June 2015 and June 2017 using floating gillnets (mesh sizes of 30-40 mm). For each sample, a total length (TL, to the nearest 0.1 cm), standard length (SL, to the nearest 0.1 cm) and total weight (TW, to the nearest 0.1 g) were recorded. The pair of lapillar otoliths

Table I. Summary of sample data.

Lake	Code	N	Standard length range (mean±SD)/mm	Standard weight range (mean±SD)/g
Bochu tsangpo	BT	40	137-300 (189.10±36.80)	34.2-362.9 (103.18±71.96)
Chargut tsangpo	CT	50	205-355 (296.24±41.26)	97.4-529.2 (284.06±144.35)
Tsachu tsangpo	TT	52	260-388 (322.08±29.76)	118.3-788.4 (459.08±129.82)
Nagtsang Co	NC	16	205-325 (260.63±35.11)	111.6-435.5 (224.54±90.79)
Kyaring Co	KC	37	302-430 (359.92±50.30)	316.3-899.2 (544.78±183.21)
Mokiu Co	MC	19	232-399 (318.00±49.86)	167.3-1370.8 (514.91±270.95)
Chargut Co	CC	22	210-375 (285.64±43.13)	105.5-643.1 (274.08±119.46)
Siling Co	SC	32	233-355 (286.44±31.67)	126.7-587 (296.01±159.87)
Uruni Co	UC	25	163-433 (247.92±81.12)	53.1-949.4 (241.53±164.64)
Yoqat Co	YC	43	257-395 (321.28±30.94)	290.7-727.8 (459.56±108.76)
Chikul Co	CK	28	247-407 (305.00±32.33)	197.6-664.1 (318.93±114.07)

Note: N, number of samples; SD, standard deviation.

(hereafter referred to as otolith) were extracted, washed with distilled water to remove any additional membranes or surface residues, air dried and stored in labelled plastic tubes.
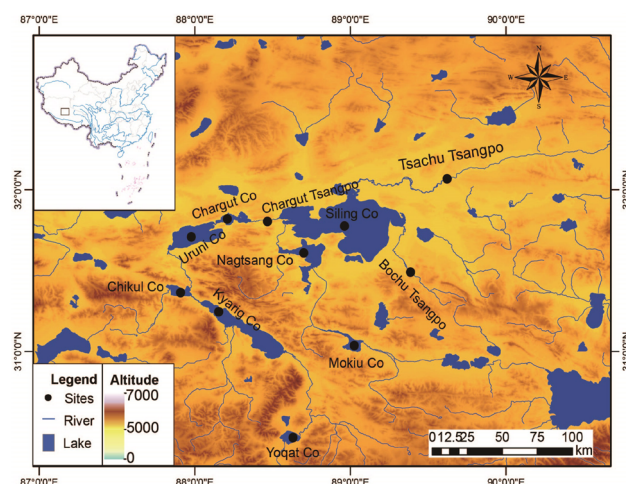

Fig. 1. Study area of northern Tibet and sampling sites (black dot).

Image and shape analysis

One side of the otolith was selected as the target material; however, one side may not always meet the requirements, as damage occasionally occurred for several otoliths on either side during the extraction procedure. Previous study used the left side of the otolith as a substitute when the right otolith was broken or unavailable (Zischke *et al*., 2016). Nevertheless, it has been suggested that differences between otoliths from two different sides must be considered in advance, and samples with damaged otoliths have to be discarded if there are significant morphometric differences between the right and left otoliths (Agüera and Brophy, 2011). Several empirical studies have shown consistent shape difference between the left and right otoliths (Mérigot *et al*., 2007; Vignon and Morat, 2010), whilst no evident differences between two sides of the otoliths were observed in the current observations (Bird *et al*., 1986; Cardinale *et al*., 2004; Ding *et al*., 2019). However, shape variation between two sides of otoliths was still unknown for *G. selincuoensis*. Thus, we performed examinations firstly to test the differences of shape descriptors between right and left otoliths. In this work, only the samples with at least one intact otolith were used for otolith measurements. Right otoliths were selected for analysis, and left otoliths were substituted only if there was no difference between two sides of otoliths.

All otoliths were weighed to the nearest 0.1 mg. High resolution images of the otoliths were captured with a digital camera (Micro Publisher 5.0 RTV) fitted to a stereo microscope (Olympus BX51; Tokyo, Japan) under appropriate magnification and using reflected light. Otoliths were put on a stage of microscope slides in a consistent manner; they were placed along the longest axis with the sulcus side up and rostrum to the right. Photographs were taken on a black background with scale bars under respective magnifications (Longmore *et al*., 2010).

Image Pro-plus 6.0 software was used to measure otolith size (area, perimeter, length, width) in otolith outlines. Length and width of each otolith was the maximum horizontal axis and maximum vertical axis of the two-dimensional images. These otolith measurements were then used to calculate the following shape indices (SDs): form-factor (FFO), circularity (CIR), rectangularity

(REC), ellipticity (ELL), roundness (RND), surface density (SDE) and aspect ratio (ARO) based on the equations proposed by Tuset *et al.* (2003) (Table II).

Table II. Size parameters and shape indices with calculation formulae for otolith of Schizothoracine.

Size parameter	Shape indices
Otolith area (OA)	Form-factor (FFO) $=4\pi OA/OP^2$
Otolith perimeter (OP)	Circularity (CIR) $= OP^2/OA$
Otolith length (OL)	Rectangularity (REC) $= OA/(OL\times OW)$
Otolith width (OW)	Ellipticity (ELL) $=(OL-OW)/(OL+OW)$
Otolith weight (OWE)	Roundness (RND) $= 4OA/\pi OL^2$
	Surface density (SDE)$=OWE/OA$
	Aspect ratio (ARO)$=OL/OW$

Note: units are mm² for OA, mm for OP, OL, OW, and mg for OWE in this paper.

In this study, the SHAPE ver 1.3 program (Iwata and Ukai, 2002) was operated to extract EFDs from the two-dimensional otolith images. In this software package, the Chain Coder program was used to describe the contours of the otoliths and stored the information as chain-codes. The Chc2Nef program generated normalized EFDs coefficients (NEFDs) of each otolith with the chain-code produced in the first step. EFDs coefficients were normalized by size and orientation, and the program gave the first three coefficients values as a1=1, b1=0, and c1=0.

The technique of elliptic Fourier analysis describes the otolith outline as harmonic. A sufficient number of harmonics have to be determined for a fish species to construct the otoliths in detail (Crampton, 1995). Cumulative percentages of Fourier Power that were calculated in previous studies were used to measure the descriptive ability of each otolith (Trojette *et al.*, 2014; Vieira *et al.*, 2014). Thus, we calculated Fourier power spectrum for *G. selincuoensis* otoliths to define the appropriate number of harmonics needed for each otolith.

Multivariate statistical analysis

SDs and NEFDs coefficients were tested for normality and homogeneity using the Kolmogorov-Smirnov normality test and Levene's test, respectively. Variables were log (x+1) transformed if they did not agree with the premises; the transformations that could not be normalized or homogenized were excluded from further analyses.

To test the variation between right and left otoliths, pairwise t-test was performed for each shape variable. The correlations of otolith shape variables with standard length among the shape variables themselves were tested by Pearson correlation analysis, and the variables that expressed significant multicollinearity were excluded. Shape variables that have significant correlations with fish size were corrected using the common within-group slope (Bergenius *et al.*, 2006; Tracey *et al.*, 2006). Analysis of Covariance (ANCOVA) was used to determine the effect of fish length on the magnitude of each shape variable. If the interaction between 'region*fish standard length' was significant, the shape variables were excluded from subsequent analyses as they could not be adjusted with fish standard length. Univariate analyses of variance (ANOVAs) were used to test the differences of shape variables between all groups. The variables that have a significant variability were adopted for discriminant analysis. Finally, permutational multivariate analysis of variance (PERMANOVA) based on Bray-Curtis distances with Monte-Carlo tests (9999 random permutations) was performed to test the significant shape difference among regions.

To evaluate the difference in otolith morphology of all stocks, two methods of statistical Non-metric Multidimensional Scaling (NMDS) and Linear Discrimination Analysis (LDA) were carried out using the descriptors mentioned above. Shape variables of SDs and NEFDs were combined for multivariate statistics. During the NMDS analysis, Euclidean distance was calculated, and the ordination plot of Euclidean distance was produced to examine separation and aggregation for inter- and intra-stocks, respectively. Stress factors were used to assess the quality of ordination that was given in the result. LDA was applied to investigate the proportion of each sample that could be correctly classified to the sites where they originally belonged. Discriminant power was assessed using Wilks' λ, which varies between 0 and 1, with zero indicating a perfect identification. To visualize the outline differences among stocks, average otolith contours were replotted by using averaged NEFDs within each group. All statistical analyses were carried out with a significance level of 0.05, and multivariable analyses were completed on SPSS (v.16.0). NMDS and LDA were performed using R statistical software (R Core Team, 2018) with the "vegan" and "MASS" R packages.

RESULTS

Image and shape analysis

A total of 364 fish individuals were sampled for morphological study, and summaries of the sample data are provided in Table I. Pairwise t-tests showed no evident shape differences between two sides of the otoliths (p>0.05) for the descriptors in Table III. A total of 364 intact otoliths, including 11 substituted individuals on the left side, were measured to obtain otolith size descriptors (Table II).

To determine the appropriate number of harmonics for *G. selincuoensis* otoliths, the cumulative variances of the harmonics were calculated with 1 to 20 harmonics. Otolith contours defined by 2, 6, 10, 14 and 18 harmonics were plotted to show the outline similarities relative to the original otolith. A total of 18 harmonics resulted in 99.99% Fourier Powers (Fig. 2). Refer to the previous studies that suggested the sufficient percentage of Fourier Power (Lord *et al*., 2012; Trojette *et al*., 2014), we used 20 harmonics to extract NEFDs and four coefficients of each harmonic were produced. Seventy-seven coefficients were used in the subsequent shape analyses since the first three coefficients ($a1=1$, $b1=0$, $c1=0$) were fixed values.
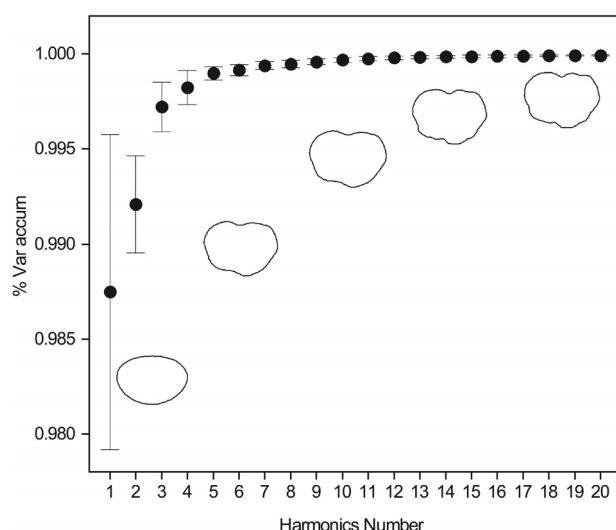

Fig. 2. Periodogram of 20 harmonics for 30 randomly selected otolith of *G. selincuoensis*. Mean (solid dots) and standard deviation (whiskers) represent the accumulated percentage of variance (% Var accum). Otolith contours shapes defined by 2,6,10,14 and 18 harmonics were plotted.

Multivariate statistical analysis

The results showed that SDs of REC and SDE variables did not achieve normality after they were transformed and were thereby removed from further analyses. A total of 80% of the numbers of NEFDs coefficients were omitted from the analysis as they could not be used (Table III). One-way univariate ANOVAs showed that the rest of the variables for SDs (FFO, CIR, ELL, RND and ARO) and NEFDs (A_4, A_5, A_{17}, A_{19}, B_3, C_6, C_7, C_{17}, D_1, D_2, D_3, D_4, and D_5) were significantly different between groups, which meant that these metrics are appropriate for discrimination analysis (Table III). The results of PERMANOVA analysis showed a significant difference between study areas using SDs and

NEFDs ($F=4.3894$, $P<0.001$).

The results of NMDS showed that otoliths from 11 regions mixed together, while using the SDs and NEFDs for scaling analysis (Fig. 3). All scatters were dispersive and did not gather according to each individual's own stock. Despite the production of low stress factors (stress factor=0.0013), the analysis of NMDS gave an inconspicuous identification for otoliths among the 11 regions.
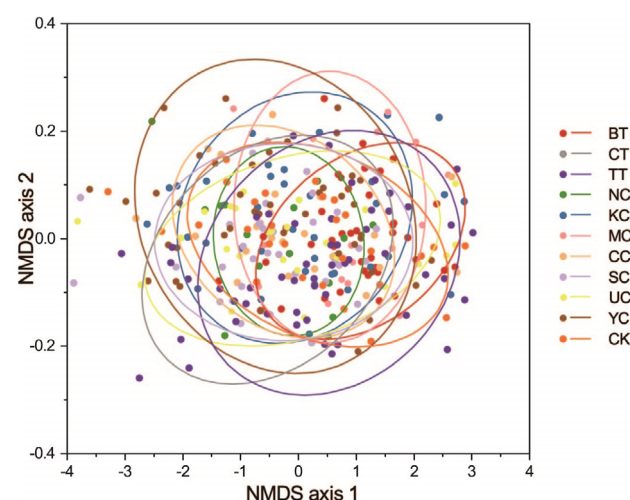

Fig. 3. Non-metric multidimensional scaling (NMDS) ordination plot of otolith from eleven stocks (stress factor =0.0013).

The scatterplot of linear discrimination showed little evidence of separation between stocks. Only group BT exhibited any possibility of being interpreted as an independent stock (Fig. 4). The first two discriminant functions explained 32.58% and 18.61% of the total variation, respectively, with levels that were significant (P<0.001). The classification matrix displayed a correct identification rate ranging from 27.3% to 70.0% (Table IV). Three stocks in rivers BT, CT and TT had successful discriminatory rates of 70.0%, 44.0% and 44.2%, respectively, and they were classified more accurately than stocks in the lakes. For example, the CC stocks possessed the highest misclassification rate of 72.7%. The discriminant analysis was significant (P<0.05) with a low Wilks' λ of 0.262, which implies stronger discriminative power. However, the overall correct classification was not very high (41.8%), which verifies that the discriminant analysis using otolith morphology did not improve the effects for *G. selincuoensis*.

Table III. Coefficients of person's correlation for variables selected for discriminate function analysis with fish standard length. Regression analysis of variables that had significant correlation with fish standard length to get the common within-group slope (*b*). One-way ANOVAs used to test the difference of variables and rectified variables between the sample regions. Pairwise t-test used to test the difference of variables between right and left otolith.

Varia-bles	Correlation analysis		Regression analysis			One-way ANOVAs		Pairwise t-test	
	t	p	F	p	b	F	p	t	p
FFO	-1.676	0.095				4.813	0.001***	-0.820	0.416
CIR	1.832	0.068				4.788	0.001***	0.730	0.730
ELL	7.912	0.001***	62.68	0.001***	2.01×10^{-4}	6.942	0.001***	-0.152	0.879
RND	7.972	0.001***	63.54	0.001***	-3.267×10^{-4}	6.913	0.001***	0.207	0.836
ARO	7.854	0.001***	61.69	0.001***	5.418×10^{-4}	7.043	0.001***	-0.167	0.867
A_4	1.576	0.116				2.112	0.023*	-0.866	0.391
A_5	4.437	0.001***	19.69	0.001***	3.484×10^{-5}	2.874	0.002**	-0.709	0.482
A_{17}	1.544	0.124				2.329	0.012*	0.212	0.833
A_{19}	2.155	0.032*	4.64	0.032*	3.276×10^{-6}	2.363	0.010**	-1.472	0.148
B_3	2.122	0.035*	4.50	0.035*	3.451×10^{-5}	2.026	0.030*	-1.316	0.195
C_6	-0.955	0.340				1.895	0.045*	-0.320	0.750
C_7	-0.464	0.643				1.938	0.039*	0.616	0.541
C_{12}	-0.189	0.851				1.977	0.035*	1.654	0.106
D_1	-6.211	0.001***	38.58	0.001***	-2.199×10^{-4}	6.961	0.001***	0.346	0.730
D_2	1.058	0.291				2.045	0.023*	0.018	0.985
D_3	-0.985	0.325				2.49	0.007**	-1.037	0.305
D_4	1.589	0.113				2.246	0.015*	-0.080	0.936
D_5	4.145	0.001***	17.18	0.001***	4.83×10^{-5}	4.707	0.001***	-0.103	0.918

FFO, form-factor; CIR, circularity; REC, rectangularity; ELL, ellipticity; RND, roundness; SDE, surface density; ARO, aspect ratio; The p-value of each predictor is given as: * $p < 0.05$; ** $p > 0.01$; *** $p < 0.001$.

Table IV. Result from linear discriminant functions of *G. selincuoensis* stocks (abbreviations of site names refer to Table 1). In rows, the numbers out brackets are quantitative proportion of otoliths classified into the sites in columns, and numbers in brackets are counts of otoliths (successful classification given in bold).

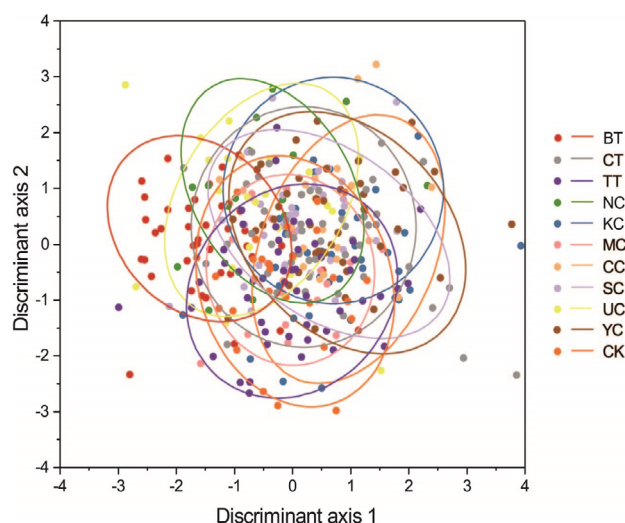| Site	Classification by shape variables											
	BT	CT	TT	NC	KC	MC	CC	SC	UC	YC	CK	Total
BT	**70.0(28)**	0.0(0)	10.0(4)	0.0(0)	0.0(0)	2.5(1)	7.5(3)	2.5(1)	2.5(1)	0.0(0)	5.0(2)	(40)
CT	6.0(3)	**44.0(22)**	8.0(4)	2.0(1)	16.0(8)	0.0(0)	4.0(2)	2.0(1)	6.0(3)	6.0(3)	6.0(3)	(50)
TT	3.8(2)	19.2(10)	**44.2(23)**	0.0(0)	5.8(3)	1.9(1)	5.8(3)	3.8(2)	3.8(2)	3.8(2)	7.7(4)	(52)
NC	18.8(3)	12.5(2)	0.0(0)	**37.5(6)**	0.0(0)	0.0(0)	6.3(1)	6.3(1)	6.3(1)	6.3(1)	6.3(1)	(16)
KC	0.0(0)	21.6(8)	13.5(5)	2.7(1)	**32.4(12)**	8.1(3)	2.7(1)	0.0(0)	2.7(1)	13.5(5)	2.7(1)	(37)
MC	0.0(0)	10.5(2)	31.6(6)	10.5(2)	0.0(0)	**36.8(7)**	0.0(0)	0.0(0)	5.3(1)	0.0(0)	5.3(1)	(19)
CC	4.5(1)	18.2(4)	9.1(2)	0.0(0)	4.5(1)	0.0(0)	**27.3(6)**	13.6(3)	0.0(0)	13.6(3)	9.1(2)	(22)
SC	3.1(1)	18.8(6)	18.8(6)	3.1(1)	0.0(0)	0.0(0)	6.3(2)	**34.4(11)**	9.4(3)	3.1(1)	3.1(1)	(32)
UC	16.0(4)	8.0(2)	4.0(1)	8.0(2)	8.0(2)	0.0(0)	0.0(0)	8.0(2)	**40.0(10)**	4.0(1)	4.0(1)	(25)
YC	4.7(2)	18.6(8)	7.0(3)	4.7(2)	9.3(4)	0.0(0)	2.3(1)	7.0(3)	4.7(2)	**37.2(16)**	4.7(2)	(43)
CK	10.7(3)	10.7(3)	32.1(9)	0.0(0)	7.1(2)	0.0(0)	0.0(0)	0.0(0)	0.0(0)	0.0(0)	**39.3(11)**	(28)

Fig. 4. Linear discriminant analysis scores for the classification of *G. selincuoensis* in northern Tibet using otolith shape variables including shape indices and Fourier descriptors. The first discriminant axis explained 32.6% variation and the second axis explained 18.6% variation (Wilks' λ = 0.263).
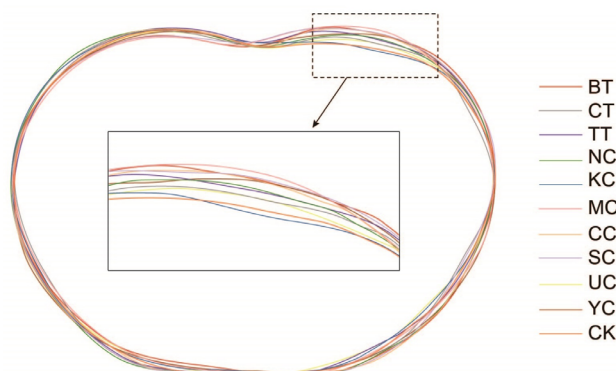

Fig. 5. The average shapes of the lapillus otolith from eleven stocks in northern Tibet. Outlines were rebuilt use average normalized elliptical Fourier coefficients within each stock. One most different area was amplified in black frame.

Average otolith outlines from each stock were repainted using average EFDs and put into a superposition as shown in Figure 5. As the figure shows, the distinctions among 11 stocks were not clearly observed, and the only minor difference appeared in the header position that is magnified in the black box. Otoliths from KC and CK had a sunken outline at the upper antirostrum side, and CT stock otoliths had deeper outlines than the other stocks on two sides of the rostrum. The differences in the outlines of each stock were congruent with variations of shape indices.

Figure 6 shows that otolith outlines in BT and MC had a relatively higher FFO but a lower RND and CIR, reflecting that these otolith outlines were more oval in shape. Stocks in TT and CK had lower ARO, which is interpreted from the relatively broad contours.
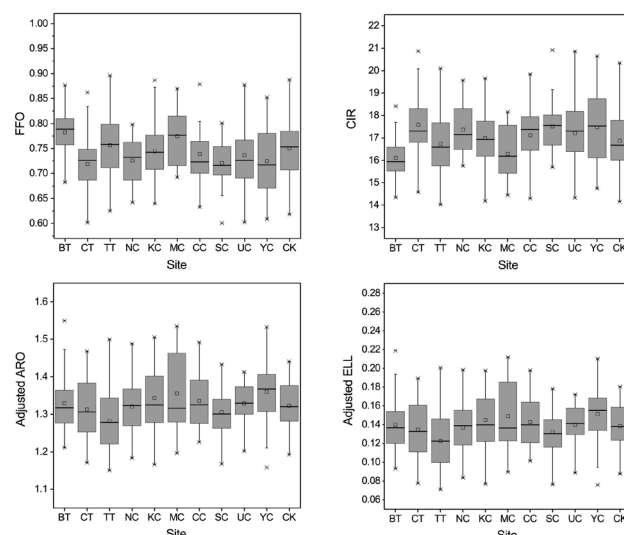

Fig. 6. Boxplots of four shape indices for eleven otolith stocks. Bold transverse line in each box represent the median value and the rectangle means average value.

DISCUSSION

Otolith shape is proven to serve as a sufficient tool for fish stock discriminations. However, lapillar otoliths are seldom used in morphological analyses since most stock discriminations are developed in marine fish species and sagittal otoliths have the most practicable outlines (Campana and Gagne, 1995). In this study, lapillar otoliths were selected for shape analysis because of their moderate size and convenient collection in species *G. selincuoensis* (Chen *et al*., 2009; Li *et al*., 2009). The results of the Elliptical Fourier analysis demonstrate that lapillar otoliths of *G. selincuoensis* can be described with limited numbers of harmonics (total of 18 harmonics explain 99.99% of the average Fourier power), suggesting that lapillar otolith shape may be potentially used for morphometric analyses. Differing from previous studies that found significant differences between left and right otoliths (Mérigot *et al*., 2007; Vignon and Morat, 2010), this study found that lapillar otoliths were the most ideal materials for fish stock discrimination for species *G. selincuoensis* because they had non-significant shape variation between two sides of the otoliths.

However, the results of the linear discriminant analysis showed that the combination of SDs and NEFDs

produced a low percent of total successful classification (41.8%), with the lowest correct classification for the CC stock (27.3%) despite a significant discriminant power produced (lower Wilks' λ value). Compared with LDA, NMDS showed a low separation degree of each stock with a small stress factor of 0.0013, indicating that a perfect fit was given. The main reason might be that dispersion of ordination had concealed the real shape variety, which is in accordance with previous study in identifying *Latris lineate* stocks (Tracey *et al.*, 2006). A series of investigations also confirmed that otolith shape analysis could be used as natural marker for stock discrimination (Agüera and Brophy, 2011; Bardarson *et al.*, 2017; Soeth *et al.*, 2019; Tracey *et al.*, 2006), and low discriminant power and high misclassification had also been obtained in other works (Cañás *et al.*, 2012; Longmore *et al.*, 2010). Presumably, the discriminant effect was associated with various factors that affected the shape variability and reduced the correct discrimination rates (Cardinale *et al.*, 2004; Vignon and Morat, 2010).

First, previous studies demonstrated that otolith shapes were mainly affected by genetic heterogeneity and environmental disparity (Stransky *et al.*, 2008b). In contrast, Vignon and Morat (2010) elucidated that otolith shape was mainly influenced by environmental variation and that genetic variation affected the otolith shape only locally. Environmental factors, such as temperature hydrogeomorphic and depth, have been confirmed as dominating influential factors on otolith shape (Ding *et al.*, 2019; Stransky *et al.*, 2008a). These factors may influence the fish's metabolism and consequently the growth rate, which changes the otolith deposition rate and results in shape variability, such as otolith length and contours (Gagliano and McCormick, 2004; Lombarte and Lleonart, 1993; Moreira *et al.*, 2019). For *G. selincuoensis,* previous studies based on D-loop sequence found low genetic divergence across different populations, which indicated low level of population genetic structure (Liang *et al.*, 2017). Besides, in northern Tibet, water temperature, depth and velocity were different between rivers and lakes, and the disparity had been proven to affect the lifestyle of Schzothoracine fishes represented of different otolith growth rate (Tao *et al.*, 2015; Tao *et al.*, 2018a). Therefore, the low successful classifications of lake stocks might be due to the homogeneity of the environmental factors among lakes. However, specific relationships between otolith morphology and environmental factors need further evaluations.

Additionally, the differences of otolith morphology among stocks had strong correlation with various feeding habits (Gagliano and McCormick, 2004). A recent study provided evidence that variations of otolith shapes were determined by dissimilar diets (Zischke *et al.*, 2016). For Schizothoracine fishes, stocks living in rivers and lakes exhibited different growth patterns since climate change affected the food source availability between the two types of water systems differently (Tao *et al.*, 2018b). Analyses on morphometrics of the feeding organ form features found that *G. selincuoensis* displayed distinct differentiations in mouth position, cornified degree of the lower jaw, gill taker number, and other features, between riverine and lacustrine stocks (Liang, 2017). Changes in feeding organs indicated that fish living in lakes for terminal months were fed mainly with aquatic insects, whereas stocks living in rivers with highly cornified lower jaws were fed attached algae (Ji, 2008). This difference of food might plasticize the otolith shapes and lead to stocks in rivers BT, CT and TT having higher correct classification rates than the other lake stocks. Meanwhile, otoliths, as a calcareous organization, play an important role in ensuring body balance for fish. In this work, relatively high percentages of correct classifications for riverine stocks illustrate that discrepancies in otolith shape may derive from adaptations to water flow features. Current studies showed that otolith shape might change in accordance with a gradient in body shape, which was associated with water flowing characteristics (Bardarson *et al.*, 2017; Haas *et al.*, 2010). Based on our results, otoliths from stocks CT, TT and BT possessed lower FFO, adjusted ARO and adjusted CIR, which suggested otoliths in rivers had a relatively slender shape compared with the otoliths in lakes. To specify the relationship between otolith shape and hydrological characteristics, more studies need to be conducted.

Furthermore, previous studies found that otolith shape analysis was not suitable for deep-water fish species stock discrimination since its slow growth characteristic could reduce otolith shape variation from different regions (DeVries *et al.*, 2002; Longmore *et al.*, 2010; Stransky, 2005). *G. selincuoensis* living in the Tibetan Plateau have the special characteristic of low growth rate (>25 years individuals which can reach up to 43 cm in length and 1.1 kg in weight) as an adaptation to the high altitude and low air temperature (Chen *et al.*, 2002). Low growth rate may dampen the divergence of growth trajectories and reduce otolith shape region-specific heterogeneity, thereby weakening the discriminant power as implied by the low total correct classification ratio (41.8%) generated in our results (Longmore *et al.*, 2010).

Finally, migrations between spawning and feeding areas also had large effects on otolith shape, which was illustrated by increasing misclassifications in stock discrimination (Zhang *et al.*, 2016). *G. selincuoensis* in northern Tibet was an anadromous species that usually migrated into rivers or freshwater lakes during its spawning period as the salty

water in SC was not suitable for eggs and larvae, and adult individuals generally lived in lakes (Ding, 2012). Based on our results, LDA showed that 18.8% individuals in the SC stock were incorrectly identified as the CT and TT stock, respectively. The reasons might be that samples in SC, CT and TT had highly mixed together, which resulted in low successful discriminant scores. Similar studies suggested that the misclassification rate increased in adjacent sites (Ibáñez *et al*., 2017), which also supported this explanation Subsequent studies should consider removing similar sites while using fewer groups for comparisons; this strategy may result in better discrimination (Ibáñez *et al*., 2017).

CONCLUSIONS

Our study performed using lapillar otolith shape in fish stock discriminant for Schizothoracine fishes in Tibet Plateau. Firstly, low shape variation between right and left otoliths suggested the usefulness of one side otolith in stock discriminant analysis. Secondly, evidence of higher correct identification rates for riverine fish stocks was derived from this study, which supports the idea that differentiation occurs between riverine and lacustrine fish stocks in accordance with previous studies on growth-increment chronologies and feeding organ features (Liang, 2017; Tao *et al*., 2018b). Moreover, additional investigations about otolith shape variation between other lakes in northern Tibet would benefit from studying environmental factors, which have significant impacts on otolith shape. To confirm the migratory trajectories, further studies are necessary to probe elemental composition in otolith layers. Studies of Schizothoracine stocks in the Siling Co basin must use other methods. Otolith shape analysis can be used as a diagnostic tool for stock discrimination because of its advantages, namely, its low cost and time-efficient, but its feasibility needs to be explored further.

ACKNOWLEDGEMENTS

Competing interests

The authors have declared no competing interests.

REFERENCES

Agüera, A. and Brophy, D., 2011. Use of saggital otolith shape analysis to discriminate Northeast Atlantic and Western Mediterranean stocks of Atlantic saury, *Scomberesox saurus saurus* (Walbaum). *Fish. Res*., **110**: 465-471. https://doi.org/10.1016/j.fishres.2011.06.003

Assis, C.A., 2007. The utricular otoliths, lapilli, of teleosts: their morphology and relevance for species identification and systematics studies. *Sci. Mar*., **69**: 259-273. https://doi.org/10.3989/scimar.2005.69n2259

Avigliano, E., Domanico, A., Sanchez, S. and Volpedo, A.V., 2017. Otolith elemental fingerprint and scale and otolith morphometry in *Prochilodus lineatus* provide identification of natal nurseries. *Fish. Res*., **186**: 1-10. https://doi.org/10.1016/j.fishres.2016.07.026

Avigliano, E., Rolón, M.E., Rosso, J.J., Mabragaña, E. and Volpedo, A.V., 2018. Using otolith morphometry for the identification of three sympatric and morphologically similar species of *Astyanax* from the Atlantic Rain Forest (Argentina). *Environ. Biol. Fish*, **101**: 1319-1328. https://doi.org/10.1007/s10641-018-0779-2

Bacha, M., Jemaa, S., Hamitouche, A., Rabhi, K. and Amara, R., 2014. Population structure of the European anchovy, *Engraulis encrasicolus*, in the SW Mediterranean Sea, and the Atlantic Ocean: evidence from otolith shape analysis. *ICES J. mar. Sci*., **71**: 2429-2435. https://doi.org/10.1093/icesjms/fsu097

Bacha, M., Jeyid, A.M., Jaafour, S., Yahyaoui, A., Diop, M. and Amara, R., 2016. Insights on stock structure of round sardinella *Sardinella aurita* off north-west Africa based on otolith shape analysis. *J. Fish Biol*., **89**: 2153-2166. https://doi.org/10.1111/jfb.13117

Bardarson, H., McAdam, B.J., Thorsteinsson, V., Hjorleifsson, E. and Marteinsdottir, G., 2017. Otolith shape differences between ecotypes of icelandic cod (*Gadus morhua*) with known migratory behaviour inferred from data storage tags. *Can. J. Fish. aquat. Sci*., **74**: 2122-2130. https://doi.org/10.1139/cjfas-2016-0307

Begg, G.A., Friedland, K.D. and Pearce, J.B., 1999. Stock identification and its role in stock assessment and fisheries management: an overview. *Fish. Res*., **43**: 1-8. https://doi.org/10.1016/S0165-7836(99)00062-

4

Begg, G.A., Overholtz, W.J. and Munroe, N.J., 2001. The use of internal otolith morphometrics for identification of haddock (*Melanogrammus aeglefinus*) stocks on Georges Bank. *Fish. Bull.*, **99**: 1-14.

Bergenius, M.A.J., Begg, G.A. and Mapstone, B.D., 2006. The use of otolith morphology to indicate the stock structure of common coral trout (*Plectropomus leopardus*) on the Great Barrier Reef, Australia. *Fish. Bull.*, **104**: 498-511.

Bian, D., Bian, B., La, B., Wang. C, Y. and Chen, T., 2010. The response of water level of selin co to climate change during 1975-2008. *Acta Geogr. Sin.*, **65**: 313-319.

Bird, J.L., Eppler, D.T. and Checkley, D.M., 1986. Comparisons of herring otoliths using fourier series shape analysis. *Can. J. Fish. aquat. Sci.*, **43**: 1228-1234. https://doi.org/10.1139/f86-152

Bostanci, D., Polat, N., Kurucu, G., Yedier, S., Kontas, S. and Darcin, M., 2015. Using otolith shape and morphometry to identify four *Alburnus* species (*A. chalcoides, A. escherichii, A. mossulensis and A. tarichi*) in Turkish inland waters. *J. appl. Ichthyol.*, **31**: 1013-1022. https://doi.org/10.1111/jai.12860

Burke, N., Brophy, D. and King, P.A., 2008. Otolith shape analysis: its application for discriminating between stocks of Irish Sea and Celtic Sea herring (*Clupea harengus*) in the Irish Sea. *ICES J. mar. Sci.*, **65**: 1670-1675. https://doi.org/10.1093/icesjms/fsn177

Campana, S.E. and Casselman, J.M., 1993. Stock discrimination using otolith shape analysis. *Can. J. Fish. aquat. Sci.*, **50**: 1062-1083. https://doi.org/10.1139/f93-123

Campana, S.E., Chouinard, G.A., Hanson, J.M., Frechet, A. and Brattey, J., 2000. Otolith elemental fingerprints as biological tracers of fish stocks. *Fish. Res.*, **46**: 343-357. https://doi.org/10.1016/S0165-7836(00)00158-2

Campana, S.E. and Gagne, J.A., 1995. Cod stock discrimination using IPCM elemental assays of otoliths. In: *Recent developments in fish otolith research*, University of South Carolina Press, Columbia SC.

Cañás, L., Stransky, C., Schlickeisen, J., Sampedro, M.P. and Fariña, A.C., 2012. Use of the otolith shape analysis in stock identification of anglerfish (*Lophius piscatorius*) in the Northeast Atlantic. *ICES J. mar. Sci.*, **69**: 250-256. https://doi.org/10.1093/icesjms/fss006

Cao, W.X., Chen, Y.F., Wu, Y.F. and Zhu, S.Q., 1981. Origin and evolution of Schizothorachine fishes in relation to the upheaval of the Xizang Plateau. In: *Studies on the period, amplitude and type of the uplift of the Qinghai-Xizang Plateau* (ed. Tibetan expedition team of the Chinese Academy of Science). Science Press, Beijing, pp. 118-130.

Cardinale, M., Doering-Arjes, P., Kastowsky, M. and Mosegaard, H., 2004. Effects of sex, stock, and environment on the shape of known-age Atlantic cod (*Gadus morhua*) otoliths. *Can. J. Fish. aquat. Sci.*, **61**: 158-167. https://doi.org/10.1139/f03-151

Che, X.H., Feng, M., Jiang, H., Xiao, T., Wang, C.Z., Jia, B. and Bai, Y., 2015. Detection and analysis of Qinghai-Tibet Plateau lake area from 2000 to 2013. *J. Geo. Inform. Sci.*, **17**: 99-107.

Chen, Y.F. and Cao, W.X., 2000. Schizothoracinae. In: *Fauna Sinica, Osteichthyes: Cypriniformes III* (ed. P.Q. Yue) Science Press, Beijing. pp. 275-390.

Chen, Y.F., Chen, Y.Y. and He, D.K., 2009. Age and growth of *Schizopygopsis younghusbandi younghusbandi* in the Yarlung Zangbo River in Tibet, China. *Environ. Biol. Fish*, **86**: 155-162. https://doi.org/10.1007/s10641-008-9370-6

Chen, Y.F., Chen, Z.M., He, D.K., Cai, B. and Ba, Z., 2001a. Hydrographic features of Sêrling Co, North Tibetan Plateau. *J. Lake Sci.*, **13**: 21-28. https://doi.org/10.18307/20010104

Chen, Y.F., He, D.K., Cao, W.X., and Duan, Z.H. 2002. Growth of Selincuo schizothoracini (*Gymnocypris selincuoensis*) in Selincuo Lake, Tibeten Platean. *Acta Zool. Sin*., **48**: 667–676.

Chen, Y.F., He, D.K. and Chen, Y.Y., 2001b. Electrophoretic analysis of isozymes and discussion about species differentiation in three species of genus *Gymnocypris*. *Zool. Res.*, **22**: 9-19.

Crampton, J.S., 1995. Elliptic fourier shape analysis of fossil bivalves: Some practical considerations. *Lethaia*, **28**: 179-186. https://doi.org/10.1111/j.1502-3931.1995.tb01611.x

DeVries, D.A., Grimes, C.B. and Prager, M.H., 2002. Using otolith shape analysis to distinguish Eastern gulf of Mexico and Atlantic Ocean stocks of king mackerel. *Fish. Res.*, **57:** 51-62. https://doi.org/10.1016/S0165-7836(01)00332-0

Ding, C., Chen, Y., He, D. and Tao, J., 2015. Validation of daily increment formation in otoliths for *Gymnocypris selincuoensis* in the Tibetan Plateau, China. *Ecol. Evol.*, **5**: 3243-3249. https://doi.org/10.1002/ece3.1572

Ding, C.Z., 2012. *Early life history of Gymnocypris selincuoensis and its adaptive mechanism to the extreme enviroment of the Qinghai-Xizang Plateau*. Ph.D thesis, The University of Chinese Academy of

Sciences, Beijing, China.

Ding, L.Y., Tao, J., Ding, C.Z., Chen, L.Q., Zhang, C., Xiang, Q.Q. and Sun, J., 2019. Hydrogeomorphic factors drive differences in otolith morphology in fish from the Nu-Salween River. *Ecol. Freshw. Fish*, **28**: 132-140. https://doi.org/10.1111/eff.12437

Dou, S., Yu, X. and Cao, L., 2012. Otolith analysis and its application in fish stock discrimination: A case study. *Oceanol. limnol. sin.*, **43**: 702-712.

Gagliano, M. and McCormick, M.I., 2004. Feeding history influences otolith shape in tropical fish. *Mar. Ecol. Prog. Ser.*, **278**: 291-296. https://doi.org/10.3354/meps278291

Haas, T.C., Blum, M.J. and Heins, D.C., 2010. Morphological responses of a stream fish to water impoundment. *Biol. Lett.*, **6**: 803-806. https://doi.org/10.1098/rsbl.2010.0401

Härkönen, T.J., 1986. *Guide to the otoliths of the bony fishes of the Northeast Atlantic*. Danbiu ApS. Biological consultants, Hellerup, Denmark. pp. 256.

He, D., Chen, Y., Liu, C., Tao, J., Ding, C. and Chen, Y., 2016. Comparative phylogeography and evolutionary history of schizothoracine fishes in the Changtang Plateau and their implications for the lake level and Pleistocene climate fluctuations. *Ecol. Evol.*, **6**: 656-674. https://doi.org/10.1002/ece3.1890

He, D.K. and Chen, Y.F., 2007. Molecular phylogeny and biogeography of highly specialized grade schizothoracine fishes (Teleostei: Cyprinidae) inferred from cytochrome *b* sequences. *Chin. Sci. Bull.*, **52**: 303-312. https://doi.org/10.1007/s11434-007-0123-2

Ibáñez, A.L., Hernandez-Fraga, K. and Alvarez-Hernandez, S., 2017. Discrimination analysis of phenotypic stocks comparing fish otolith and scale shapes. *Fish. Res.*, **185**: 6-13. https://doi.org/10.1016/j.fishres.2016.09.025

Ihssen, P.E., Booke, H.E., Casselman, J.M., Mcglade, J.M., Payne, N.R. and Utter, F.M., 1981. Stock identification: materials and methods. *Can. J. Fish. aquat. Sci.*, **38**: 1838-1855. https://doi.org/10.1139/f81-230

Iwata, H. and Ukai, Y., 2002. SHAPE: A computer program package for quantitative evaluation of biological shapes based on Elliptic Fourier descriptors. *J. Hered.*, **93**: 384-385. https://doi.org/10.1093/jhered/93.5.384

Ji, Q., 2008. *The study on the morphology of feeding organs and the feeding habitats of six Schizothoracine fishes*. Master's thesis. Huazhong Agricultural University, Wuhan, Hubei, China.

Jia, Y.T. and Chen, Y.F., 2009. Otolith microstructure

of *Oxygymnocypris stewartii* (Cypriniformes, Cyprinidae, Schizothoracinae) in the Lhasa River in Tibet, China. *Environ. Biol. Fish*, **86**: 45-52. https://doi.org/10.1007/s10641-008-9334-x

Kuhl, F.P. and Giardina, C.R., 1982. Elliptic Fourier features of a closed contour. *Comput. Vision. Graph.*, **18**: 236-258. https://doi.org/10.1016/0146-664X(82)90034-X

Li, X.Q., Chen, Y.F., He, D.K. and Chen, F., 2009. Otolith characteristics and age determination of an endemic *Ptychobarbus dipogon* Regan, 1905) (Cyprinidae: Schizothoracinae) in the Yarlung Tsangpo River, Tibet. *Environ. Biol. Fish.*, **86**: 53-61. https://doi.org/10.1007/s10641-008-9420-0

Liang, Y., He, D., Jia, Y., Sun, H. and Chen, Y., 2017. Phylogeographic studies of schizothoracine fishes on the central Qinghai-Tibet Plateau reveal the highest known glacial microrefugia. *Sci. Rep-UK.*, **7**: 10983. https://doi.org/10.1038/s41598-017-11198-w

Liang, Y.Y., 2017. *Speciation and phylogeography of schizothoracine fishes in Siling Co Basin, north Tibetan Plateau*. Ph.D thesis, The University of Chinese Academy of Sciences, Beijing, China.

Lombarte, A. and Lleonart, J., 1993. Otolith size changes related with body growth, habitat depth and temperature. *Environ. Biol. Fish.*, **37**: 297-306. https://doi.org/10.1007/BF00004637

Longmore, C., Fogarty, K., Neat, F., Brophy, D., Trueman, C., Milton, A. and Mariani, S., 2010. A comparison of otolith microchemistry and otolith shape analysis for the study of spatial variation in a deep-sea teleost, *Coryphaenoides rupestris*. *Environ. Biol. Fish.*, **89**: 591-605. https://doi.org/10.1007/s10641-010-9674-1

Lord, C., Morat, F., Lecomte-Finiger, R. and Keith, P., 2012. Otolith shape analysis for three *Sicyopterus* (Teleostei: Gobioidei: Sicydiinae) species from new Caledonia and Vanuatu. *Environ. Biol. Fish.*, **93**: 209-222. https://doi.org/10.1007/s10641-011-9907-y

Ma, R., Yang, G., Duan, H., Jiang, J., Wang, S., Feng, X., Wang, S., Feng, X., Li, A., Kong, F., Xue, B., Wu, J. and Li, S., 2011. China's lakes at present: Number, area and spatial distribution. *Sci. China Earth Sci.*, **54**: 283-289. https://doi.org/10.1007/s11430-010-4052-6

Mérigot, B., Letourneur, Y. and Lecomte-Finiger, R., 2007. Characterization of local populations of the common sole solea solea (Pisces, Soleidae) in the NW Mediterranean through otolith morphometrics and shape analysis. *Mar. Biol.*, **151**: 997-1008. https://doi.org/10.1007/s00227-006-0549-0

Moreira, C., Froufe, E., Vaz-Pires, P. and Correia, A.T., 2019. Otolith shape analysis as a tool to infer the population structure of the blue jack mackerel, *Trachurus picturatus*, in the NE Atlantic. *Fish. Res.*, **209**: 40-48. https://doi.org/10.1016/j.fishres.2018.09.010

Neves, A., Sequeira, V., Farias, I., Vieira, A.R., Paiva, R. and Gordo, L.S., 2011. Discriminating bluemouth, *Helicolenus dactylopterus* (Pisces: Sebastidae), stocks in Portuguese waters by means of otolith shape analysis. *J. mar. Biol. Assoc. U.K.*, **91**: 1237-1242. https://doi.org/10.1017/S002531541000189X

R Core Team, 2018. *R: A language and environment for statistical computing*. R Foundation for Statistical Computing, Vienna, Austria. https://www.R-project.org/.

Secor, D.H., 2013. The unit stock concept: Bounded fish and fisheries. In: *Stock identification methods* (eds. S.X. Cadrin, L.A. Kerr and S. Mariani), 2ᵗʰ ed. Academic Press, New York, pp. 7-28. https://doi.org/10.1016/B978-0-12-397003-9.00002-3

Soeth, M., Spach, H.L., Daros, F.A., Adelir-Alves, J., de Almeida, A.C.O. and Correia, A.T., 2019. Stock structure of atlantic spadefish *Chaetodipterus faber* from Southwest Atlantic Ocean inferred from otolith elemental and shape signatures. *Fish. Res.*, **211**: 81-90. https://doi.org/10.1016/j.fishres.2018.11.003

Stransky, C., 2005. Geographic variation of golden redfish (*Sebastes marinus*) and deep-sea redfish (*S. mentella*) in the north atlantic based on otolith shape analysis. *ICES J. mar. Sci.*, **62**: 1691-1698. https://doi.org/10.1016/j.icesjms.2005.05.012

Stransky, C., Baumann, H., Fevolden, S.E., Harbitz, A., Hoie, H., Nedreaas, K.H., Salberg, A. B. and Skarstein, T.H., 2008a. Separation of Norwegian coastal cod and Northeast Arctic cod by outer otolith shape analysis. *Fish. Res.*, **90**: 26-35. https://doi.org/10.1016/j.fishres.2007.09.009

Stransky, C., Murta, A.G., Schlickeisen, J. and Zimmermann, C., 2008b. Otolith shape analysis as a tool for stock separation of horse mackerel (*Trachurus trachurus*) in the Northeast Atlantic and Mediterranean. *Fish. Res.*, **89**: 159-166. https://doi.org/10.1016/j.fishres.2007.09.017

Tao, J., Chen, Y., He, D. and Ding, C., 2015. Relationships between climate and growth of *Gymnocypris selincuoensis* in the Tibetan Plateau. *Ecol. Evol.*, **5**: 1693-1701. https://doi.org/10.1002/ece3.1463

Tao, J., He, D., Kennard, M.J., Ding, C., Bunn, S.E., Liu, C., Jia, Y., Che, R. and Chen, Y., 2018a. Strong evidence for changing fish reproductive phenology under climate warming on the Tibetan Plateau. *Global Change Biol.*, **24**: 2093-2104. https://doi.org/10.1111/gcb.14050

Tao, J., Kennard, M.J., Jia, Y. and Chen, Y., 2018b. Climate-driven synchrony in growth-increment chronologies of fish from the world's largest high-elevation river. *Sci. Total Environ.*, **645**: 339-346. https://doi.org/10.1016/j.scitotenv.2018.07.108

Torres, G.J., Lombarte, A. and Morales-Nin, B., 2000. Sagittal otolith size and shape variability to identify geographical intraspecific differences in three species of the genus *Merluccius*. *J. mar. Biol. Assoc. U.K.*, **80**: 333-342. https://doi.org/10.1017/S0025315499001915

Tracey, S.R., Lyle, J.M. and Duhamel, G., 2006. Application of elliptical Fourier analysis of otolith form as a tool for stock identification. *Fish. Res.*, **77**: 138-147. https://doi.org/10.1016/j.fishres.2005.10.013

Trojette, M., Fatnassi, M., Ben Alaya, H., Mahouachi, N.E.H., Chalh, A., Quignard, J.-P. and Trabelsi, M., 2014. Applying Sagitta otolith shape in the discrimination of fish populations *Scorpaena porcus* (Linnaeus, 1758) (Scorpaenidae) in the Tunisian coasts. *Cah. Biol. Mar.*, **55**: 499-506.

Tuset, V.M., Lozano, I.J., Gonzalez, J.A., Pertusa, J.F. and Garcia-Diaz, M.M., 2003. Shape indices to identify regional differences in otolith morphology of comber, *Serranus cabrilla* (L., 1758). *J. appl. Ichthyol.*, **19**: 88-93. https://doi.org/10.1046/j.1439-0426.2003.00344.x

Tuset, V.M., Rosin, P.L. and Lombarte, A., 2006. Sagittal otolith shape used in the identification of fishes of the genus *Serranus*. *Fish. Res.*, **81**: 316-325. https://doi.org/10.1016/j.fishres.2006.06.020

Vieira, A., Neves, A., Sequeira, V., Paiva, R.B. and Gordo, L.S., 2014. Otolith shape analysis as a tool for stock discrimination of forkbeard (*Phycis phycis*) in the Northeast Atlantic. *Hydrobiology*, **728**: 103-110. https://doi.org/10.1007/s10750-014-1809-5

Vignon, M. and Morat, F., 2010. Environmental and genetic determinant of otolith shape revealed by a non-indigenous tropical fish. *Mar. Ecol. Prog. Ser.*, **411**: 231-241. https://doi.org/10.3354/meps08651

Wu, Y.F. and Wu, C.Z., 1992. *The fishes of the Qinghai-Xizang Plateau*. Sichuan Publishing House of Science and Technology, Chengdu, China.

Zhang, C., Ye, Z.J., Li, Z.G., Wan, R., Ren, Y.P. and Dou, S.Z., 2016. Population structure of Japanese Spanish mackerel *Scomberomorus niphonius* in the Bohai Sea, the YellowSea and the East China Sea: Evidence from random forests based on otolith features. *Fish. Sci.*, **82**: 251-256. https://doi.org/10.1007/s12562-

016-0968-x

Zischke, M.T., Litherland, L., Tilyard, B.R., Stratford, N.J., Jones, E.L. and Wang, Y.G., 2016. Otolith morphology of four mackerel species (*Scomberomorus* spp.) in Australia: Species differentiation and prediction for fisheries monitoring and assessment. *Fish. Res.*, **176**: 39-47. https://doi.org/10.1016/j.fishres.2015.12.003